

Sewer and Culvert Deterioration and its Implications for Design of Liners

Ian D. Moore

GeoEngineering Centre at Queen's-RMC, Queen's University, Kingston, Canada

ABSTRACT

Rigid sewer pipes and metal culverts are examined, considering deterioration of the pipe structure and the surrounding backfill. Changes to factor of safety are assessed as a result of steel corrosion and soil erosion, and the deformations of corroded metal and fractured concrete and clay pipes are also quantified. The effects of these forms of deterioration on the performance of liners are then considered, examining resistance to both external earth and fluid loads on liners. Simplified design equations are presented to quantify the deformations expected under earth loads, and the effect of pipe and soil deterioration on the resistance of liners to buckling and bending.

1. INTRODUCTION

Methods of rigid pipe repair have been actively under development and use for decades and much is known regarding the resistance of polymer sewer liners to both external fluid loads (e.g. El Sawy and Moore, 1997) and external earth loads (e.g. Law and Moore, 2007). Video (closed circuit television or CCTV) inspection is used routinely to determine the extent of the damage visible within the sewer (Figure 1a), and many standards exist to guide the design of liners for insertion within the sewer (e.g. ASTM F1216-06).

While it might seem that there is little need for further research on these topics, the processes by which the stability of rigid and flexible pipes change over time (e.g. Tan and Moore, 2007; El Taher and Moore, 2008), and the role of soil erosion on fracture of rigid pipes are only now being studied (e.g. Spasojevic et al., 2006).



a. Fractured Clay Sewer in Toronto.



b. Corroded metal culvert in Eastern Ontario

Figure 1. Typical damage of structures requiring repair.

It is clear that the deterioration of soil support around a rigid pipe is the most critical feature leading to the structural damage visible during video inspections, and it is understood that fractured or corroded sewers and culverts before and after repair have stability dependent on the composite action of the soil (intact or deteriorated), the damaged pipe, and the liner within (e.g. Law and Moore, 2007). These recent findings are used here to determine what can be inferred from the extent of damage seen during inspections, and to examine how the likely consequences of both pipe and soil deterioration can be taken into consideration in the design of sewer repairs.

2. FRACTURE AND DEFORMATION OF RIGID PIPE DUE TO SOIL EROSION

While it is difficult to obtain images of erosion voids, it is reasonably certain that critical voids can develop at the springline of rigid and flexible culverts, Figure 2a. These develop long before they are sufficiently large to produce sinkholes or other features visible at the ground surface. Furthermore, experiments reported by Spasojevic et al. (2006) indicate that voids at the invert are filled by soil moving down from the springlines, so that the final result is loss of lateral support.

Tan and Moore (2007) used finite element analyses to examine the stresses within a rigid sewer pipe as voids grow at the springline. Figure 2b shows a typical mesh used in their study, with three different sized circular zones at the springline used to model progressive growth of the void, Figure 2c. They found that the primary geometrical variable controlling pipe deformation is the angle of contact α between the void and the outside of the pipe.

Tan and Moore (2007) also used finite element analysis to calculate the deformations (decreases in vertical pipe diameter, and increases in horizontal pipe diameter) that then result after the pipe fractures. Idealizing the fractured pipe, Figure 3a, as four quadrants, Figure 3b, finite element analysis was used by Tan (2007) to calculate pipe response, Figure 4. Following comparison with the kinematics of fracture pipe deformation (Law and Moore, 2007), it was found that the fractured pipe responds much like a flexible pipe, so that changes in horizontal pipe diameter are:

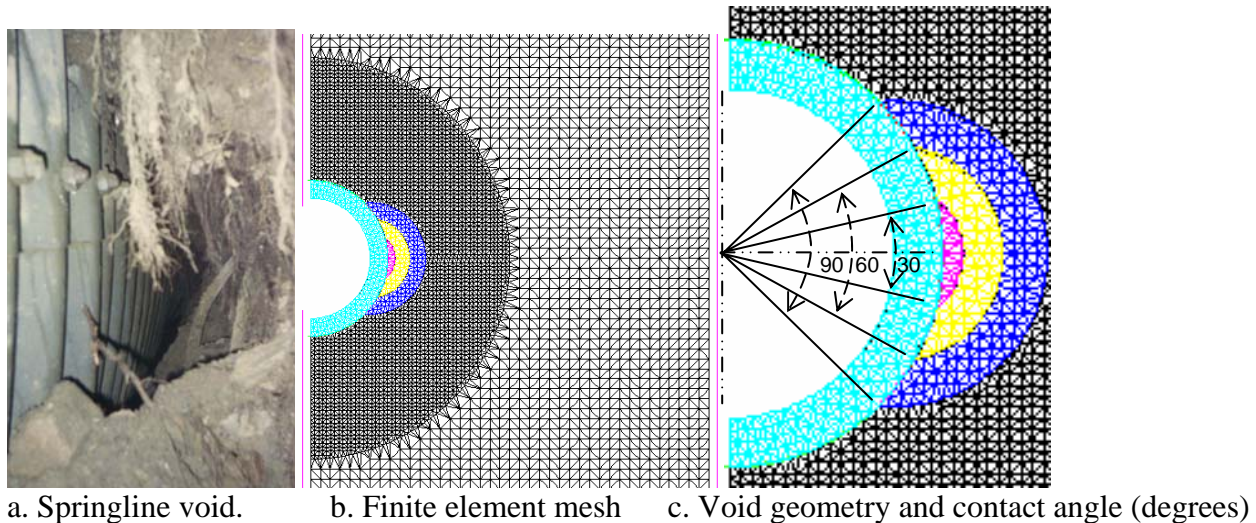
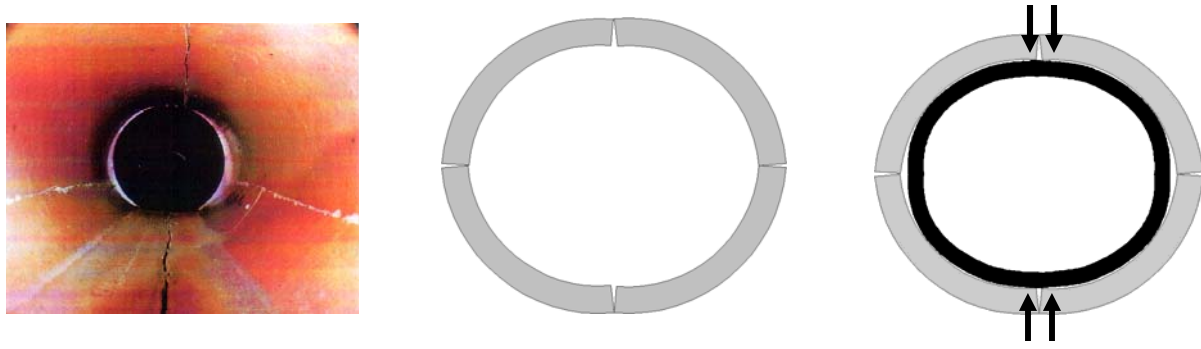


Figure 2. Finite element analysis considering erosion voids (after Tan and Moore, 2007).



a. Fractured German sewer b. Fracture pattern and kinematics c. Response of liner
 Figure 3. Four segment hinge mechanism for rigid pipe after fracturing (Moore, 2005).

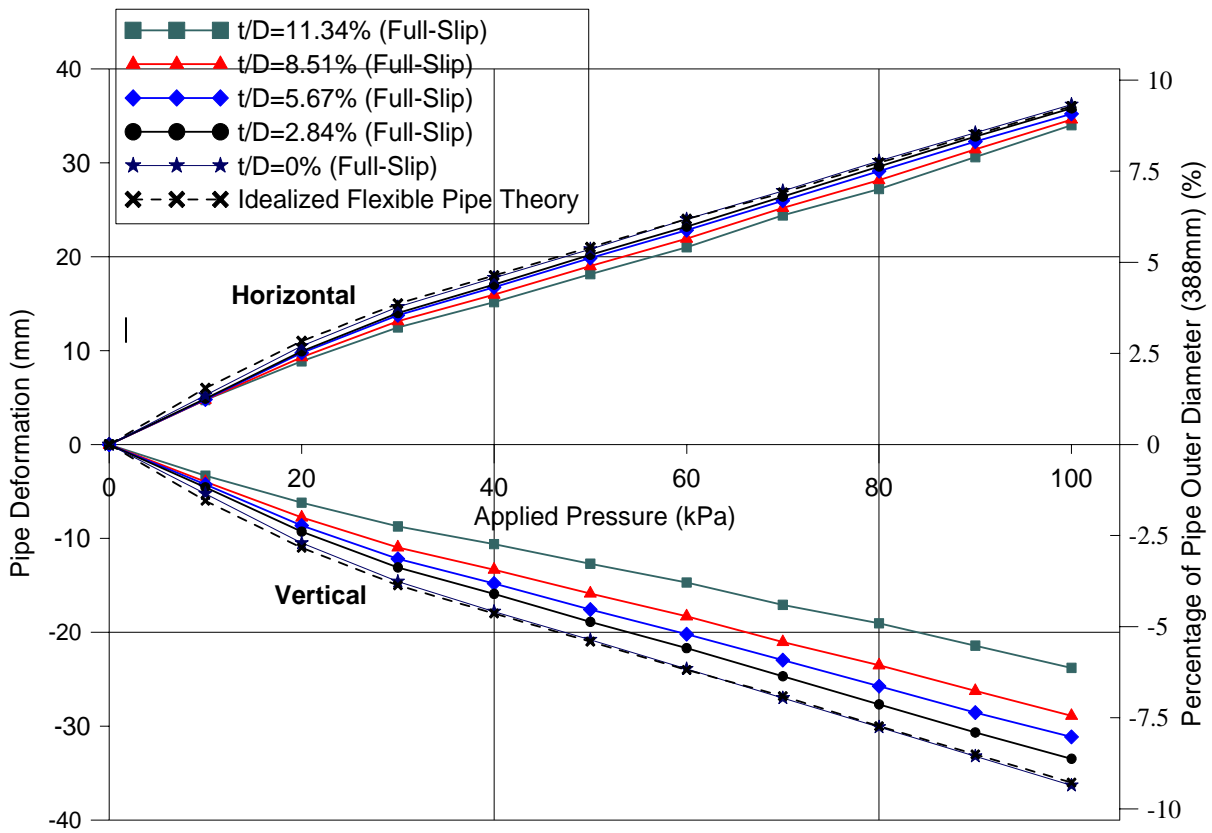


Figure 4. Fractured pipe deformation versus overburden (finite element analysis and flexible pipe theory), Tan (2007).

$$\Delta D_H / ID_{pipe} \approx 1.6 \frac{\sigma_v}{M_s} \left(1 + \frac{2t_{pipe}}{ID_{pipe}} \right) \quad [1]$$

where overburden stress σ_v , lateral earth pressure ratio K , constrained modulus M_s and Poisson's ratio of the soil ν_s all influence the response, and the expression 1.6 is based on $K=0.45$, and $\nu_s=0.3$. Other combinations of K and ν_s result in values ranging from 1.4 to 1.7. The kinematics of pipe deformation can then be used to provide a relationship between changes in vertical and horizontal diameters:

$$\Delta D_V = -\Delta D_H \cdot \left(1 - \frac{2 \cdot t_{pipe}}{OD_{pipe}}\right) \quad [2]$$

Combining equations 1 and 2, the relationship is obtained between the secant value of constrained soil modulus M_s , (the modulus relating total change in pipe diameter to total value of vertical overburden stress), the change in vertical pipe diameter $\Delta D_v/ID_{pipe}$, and the depth of burial of the pipe. Figure 5 shows this for a fractured or flexible pipe in intact (not eroded) soil. This figure also includes expected values of modulus for various backfill materials, McGrath et al. (2002), which will be used in a subsequent section to assess the extent of erosion void.

Further finite element analyses of fractured pipe deformations were conducted, examining the increase in pipe deformations as erosion voids like those seen in Figure 2c develop at the springlines. Figure 6 presents the resulting calculations based on either elastic soil response, or elastic-plastic soil response (where shear failure in the soil around the void is considered). These calculations were performed for a fine grained backfill, where coefficient of lateral earth pressure is either $K=0.5$ or $K=0.67$. Shear strength in the elastic-plastic analysis is considered to be drained, using an angle of internal friction for the fine grained soil of $\phi=20^\circ$. These results will also be used in a subsequent section to characterise the soil condition.

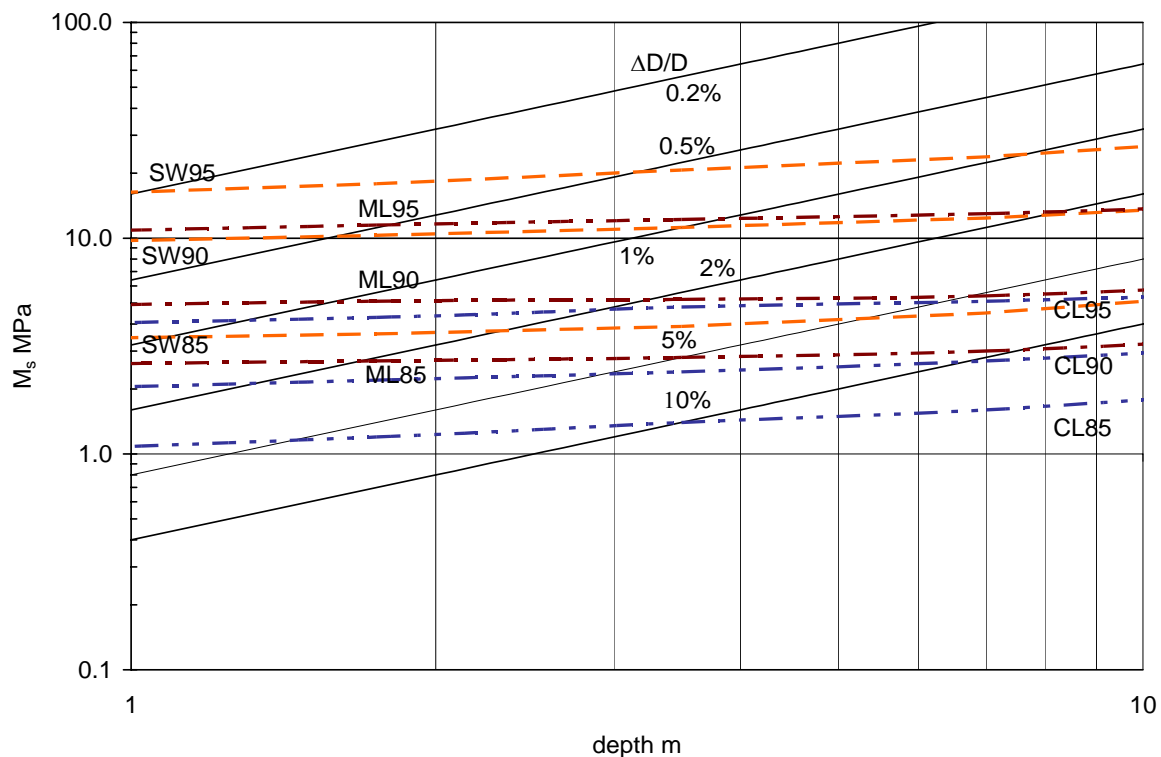


Figure 5. Soil modulus and flexible or fractured pipe deformations as a function of burial depth.

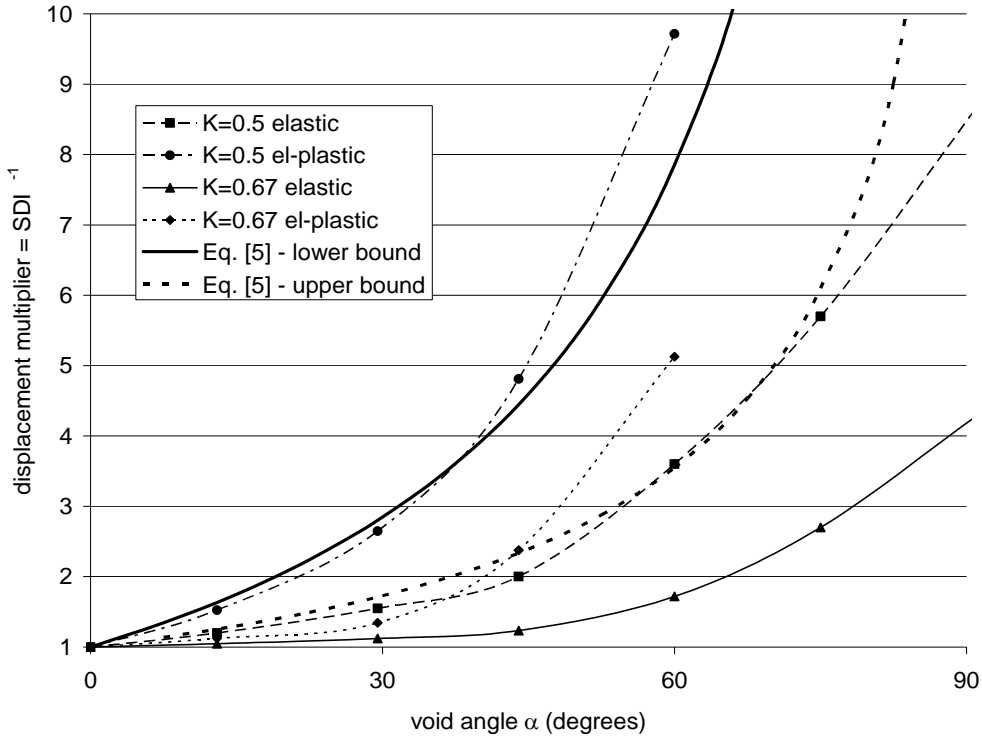
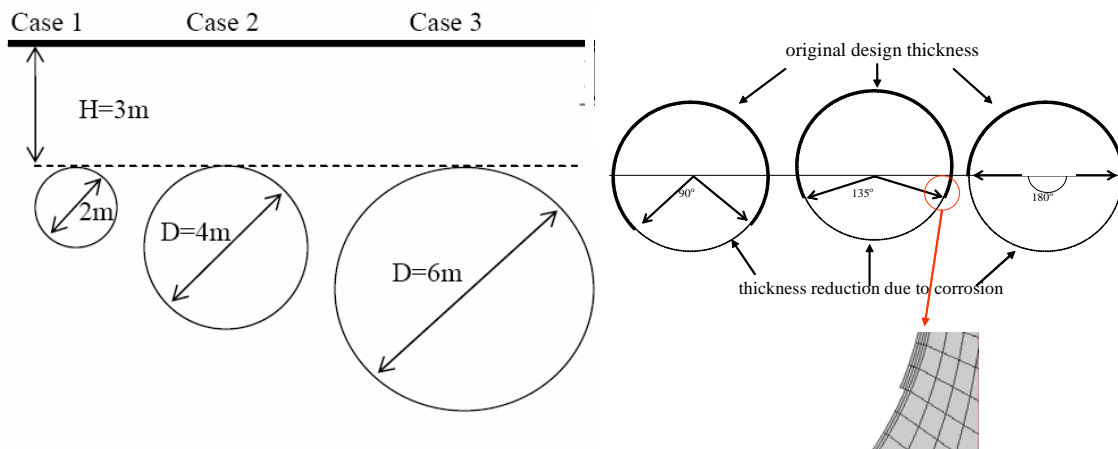


Figure 6. Proportional displacement increase due to erosion void of contact angle α .

3. STABILITY ASSESSMENT OF CORRODED METAL CULVERTS

Finite element analysis has also been used to study the stability of corroded metal culverts, El Taher and Moore (2008). This study considered corrugated metal culverts of three different diameters, composed of 152mm x 52mm corrugated steel plate, Figure 7a. Initial pipe thicknesses were chosen to satisfy current North American design standards like AASHTO, and then culvert responses were calculated resulting from reductions in wall thickness across three different angles from the invert, Figure 7b.



a. Geometry of the circular metal culverts b. Extent of uniform wall loss across the invert
Figure 7. Deteriorated culvert problems considered by El Taher and Moore (2008).

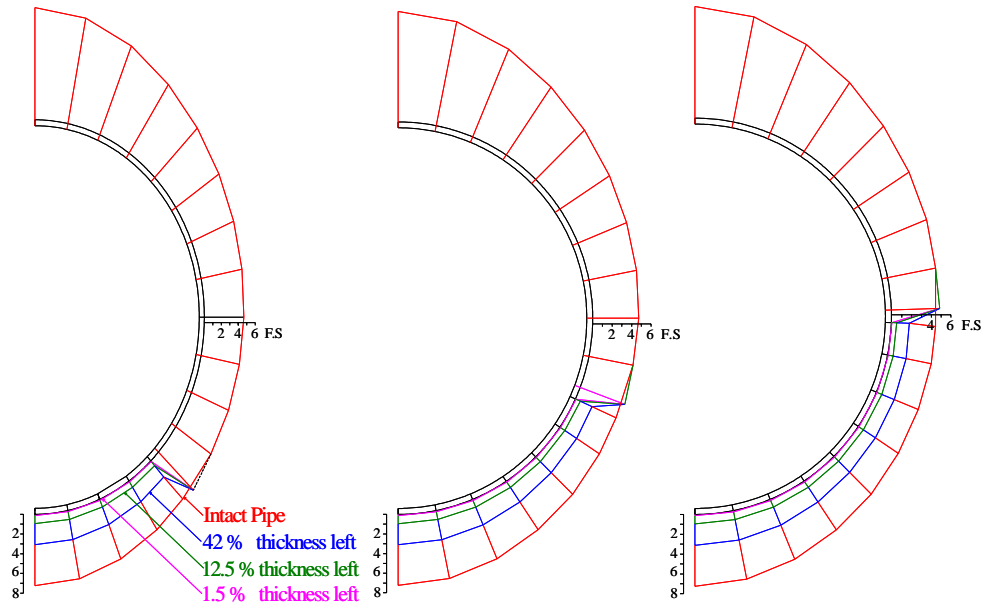


Figure 8. Factor of safety against yield for corroded culvert (case 2), El Taher and Moore (2008).

Figure 8 shows factor of safety against yield in the steel structure calculated around the circumference for Case 2. In each case, there is a substantial decrease in factor of safety in the corroded plate, at the position where it meets the intact structure. Figure 9 presents these changes in factor of safety against yield at the junction between the corroded and uncorroded sections as a function of the amount of plate thickness that remains, and governing factor of safety is the lesser of this and that at the location of maximum thrust (the springline). For all cases considered, the factor of safety decreases linearly with wall thickness. These calculations reflect the fact that the thrusts and moments in the structure barely change as the wall corrodes.

Unless the surrounding soil degrades, the structural deformations are likely small. The culvert is already flexible in bending relative to the soil, and remains stiff in hoop compression unless wall loss is almost complete, so there is no significant change in relative stiffness. If soil modulus changes before lining, deformations for a circular structure could be estimated using Figure 6. Work is currently underway to study the effect of soil erosion on metal culvert stability.

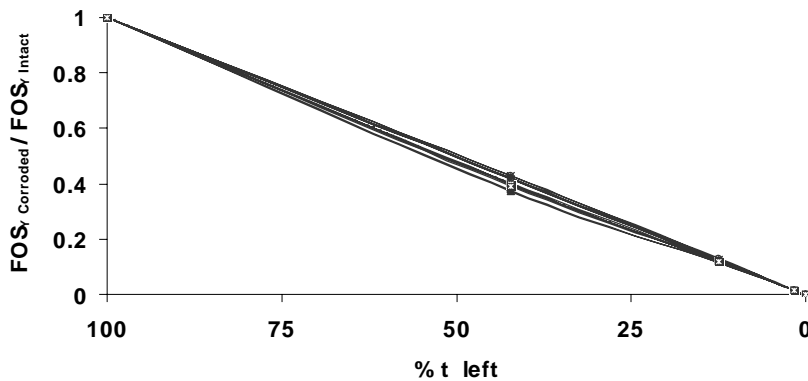


Figure 9. Change in factor of safety against yield calculated just within the corroded zone (all cases), El Taher and Moore (2008).

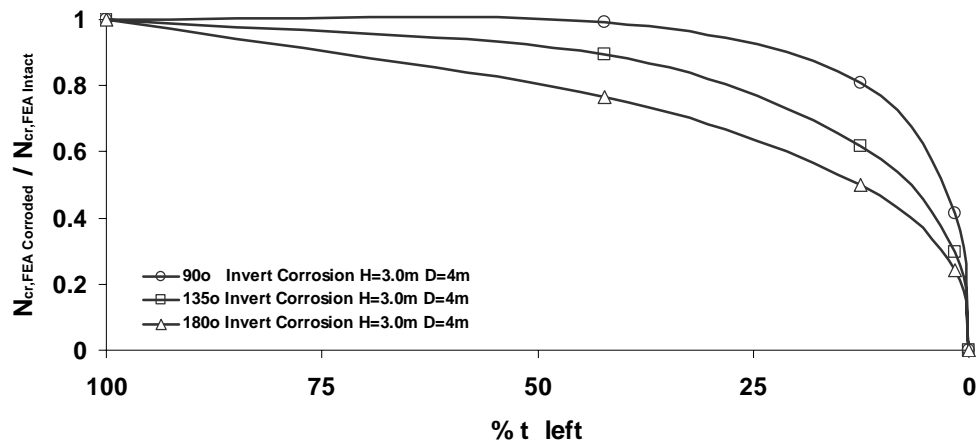


Figure 10. Change in factor of safety against buckling due to corrosion (Case 2), El Taher and Moore (2008).

Figure 10 summarizes the effect of corrosion on culvert buckling strength. These indicate that there is little change in resistance to buckling until less than half of the thickness remains. After that point, stability reductions accelerate. As expected, reductions in buckling strength are greater for the case where wall thickness loss extends from Springline to Springline. However, for these culverts with good soil support, yield is the governing limit state.

4. INTERPRETATION OF SOIL CONDITION – DETERIORATED MODULUS

Figure 5 can be used to estimate the current soil condition around the damaged sewer.

- i. If the soil material used in original sewer construction is known, then the amount of deformation for a fractured rigid pipe within intact (not deteriorated) ground can be obtained from the figure, $(\Delta D_v / ID_{pipe})_{intact}$.
- ii. The actual level of observed deformation $(\Delta D_v / ID_{pipe})_{CCTV}$ can then be used to define a soil degradation index:

$$SDI = (\Delta D_v / ID_{pipe})_{CCTV} / (\Delta D_v / ID_{pipe})_{intact} \quad [3]$$

- iii. While soil erosion is expected to develop in a nonuniform manner, with greater degradation in some areas, and less in others, a single equivalent degraded soil modulus can be found from the figure, based on the depth of burial and the level of observed deformation in the fractured pipe, $(\Delta D_v / ID_{pipe})_{CCTV}$.
- iv. The ratio of the intact soil modulus and the equivalent degraded modulus can also be used to define the soil degradation index

$$SDI = M_{S,equivalent} / M_{S,intact} \quad [4]$$

5. INTERPRETATION OF SOIL CONDITION – VOID SIZE

Using the relationships between void size and pipe deformation discussed earlier in section 2 in relation to Figure 6, the size of the void can be estimated from the soil degradation index (that is, the amount of deflection observed in a CCTV inspection). Curve fitting to the relationships

shown on Figure 6, an expression has been developed between deflection increase and the size of the erosion void α :

$$(SDI)^{-1} = \frac{A + B\alpha}{A - \alpha} \quad \alpha = \frac{A(SDI^{-1} - 1)}{B + SDI^{-1}} \quad [5]$$

Two parameter sets were selected for the results presented in Figure 6:

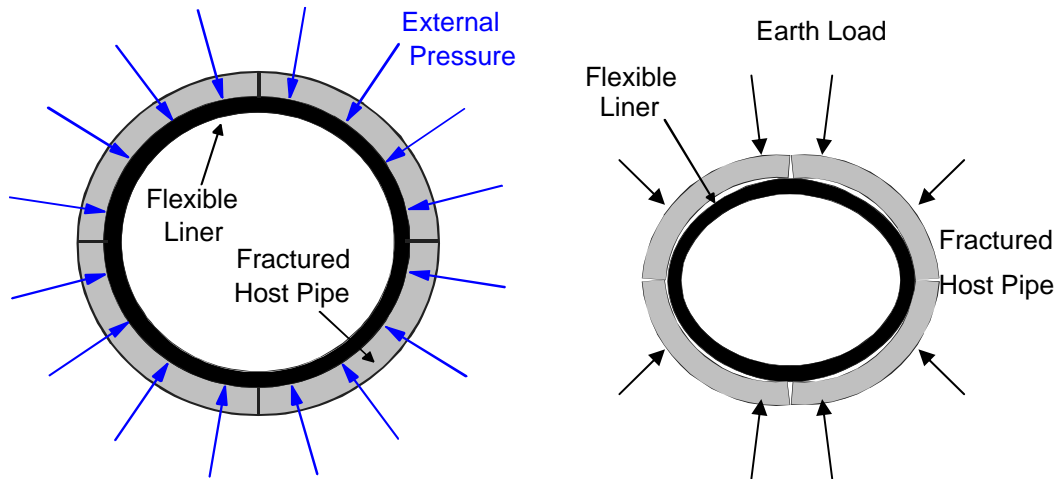
- i. one providing 'lower bound' void size for a given level of displacement increase; these correspond to results for elastic-plastic ground and $K = 0.5$, $A = 95$, $B = 3$; and
- ii. one providing 'upper bound' void size for a given level of displacement increase; these correspond to results for a stronger material and/or one where $K = 0.67$, $A = 100$, $B = 0.7$.

Figure 6 includes these two curve fits from Eq. [5]. These parameters provide only preliminary estimates of void size. Experimental results are needed to evaluate these theoretical calculations.

6. INFLUENCE OF PIPE AND SOIL CONDITIONS ON LINER DESIGN

6.1 Performance limits for liner within gravity flow sewer

There are two performance limits that need to be considered when designing the polymer liner. First, the liner needs to be able to support the external fluid pressures in the surrounding ground without buckling, Figure 11a. Second, the liner needs to withstand tensile bending strains at crown and invert as the vertical diameter of the fractured sewer decreases under the influence of the earth loading, Figure 11b (see also Figure 3c where the interaction forces are illustrated).



a. Liner under external groundwater pressure b. Liner bending as vertical diameter decreases
Figure 11. Performance limits for liner within gravity flow sewer, Moore (2005).

6.2 Reductions in buckling strength

For a close-fitting liner, Moore (2005) indicates that the buckling pressure is given by

$$P_b = 1.0E_{liner} \left(\frac{t_{liner}}{D_{liner}} \right)^{2.2} R_q R_\Delta \quad [6]$$

where R_q and R_Δ are correction factors accounting for pipe ovality q and a small wavy imperfection in the liner of amplitude Δ . Ovality for a fractured circular sewer is:

$$q = \frac{D_H - D_V}{D_H + D_V} \approx \frac{\Delta D_H}{ID_{pipe}} \quad [9]$$

if the effect of the thickness of the old sewer is neglected (which will be conservative).

If the liner drapes over a fractured rigid sewer at the invert, Figure 11b, amplitude is given by

$$\Delta \approx 0.5 ID_{pipe} \left(\frac{\Delta D_H}{ID_{pipe}} \right)^2 \left(1 + \frac{2t_{pipe}}{ID_{pipe}} \right)^{-1} \quad [10]$$

where ID_{pipe} is the internal diameter of the uncracked sewer. This can be further simplified by ignoring the thickness of the old sewer (providing a conservative approximation).

Using expressions for reduction factors quantified by El Sawy and Moore (1997), reduction in stability as a result of deformations in the fractured sewer are given by

$$R_q R_\Delta = e^{-q/0.18} e^{-0.56\Delta/t_{liner}} = e^{-\Delta D_H / 0.18 ID_{pipe}} e^{-0.28 \frac{ID_{pipe}}{t_{liner}} \left(\frac{\Delta D_H}{ID_{pipe}} \right)^2} \quad [11]$$

The magnitude of this reduction is illustrated in Figure 12 for a range of dimension ratios $DR=D/t$ of the liner and changes in horizontal pipe diameter.

Initial corroded metal culvert shape may be noncircular, influencing liner buckling. Other changes in buckling strength are not expected unless soil degradation produces deformation.

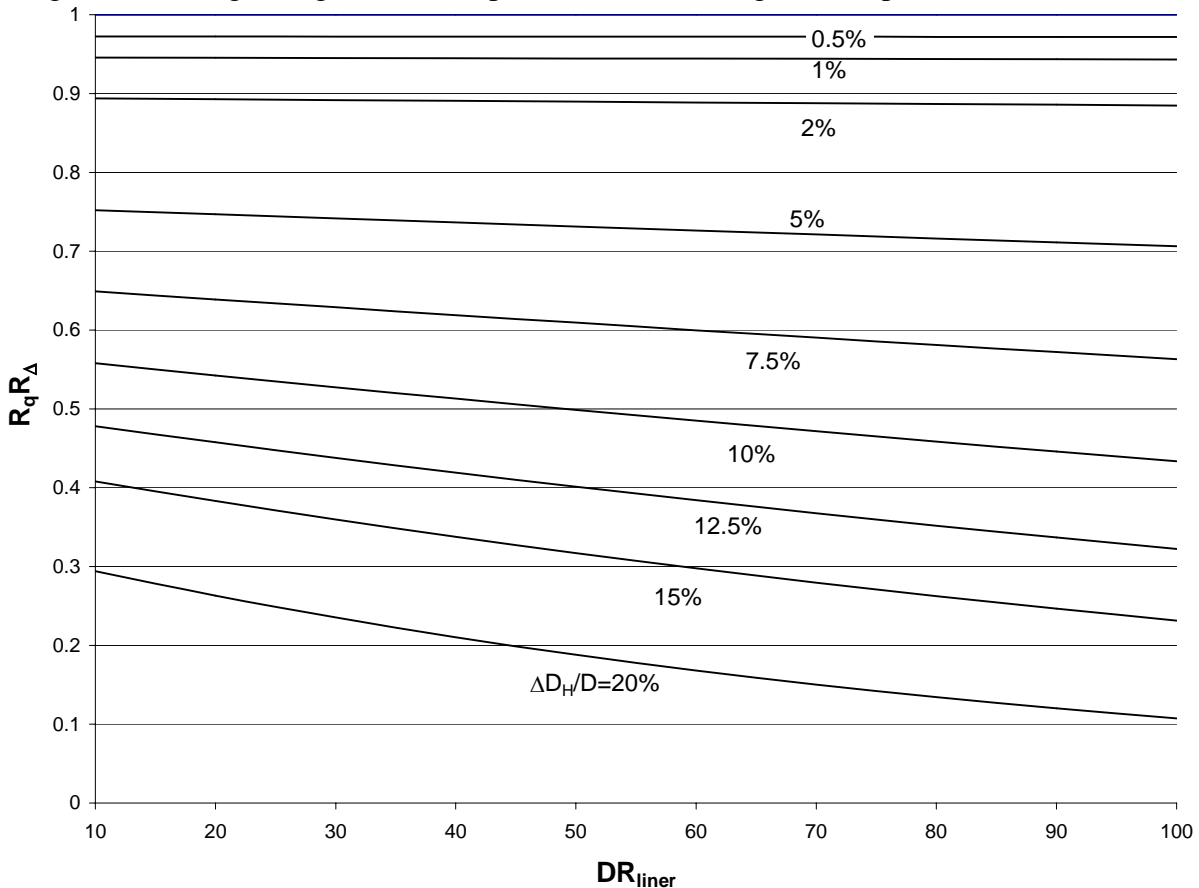


Figure 12. Buckling strength reduction factor for fractured sewer with close fitting liner

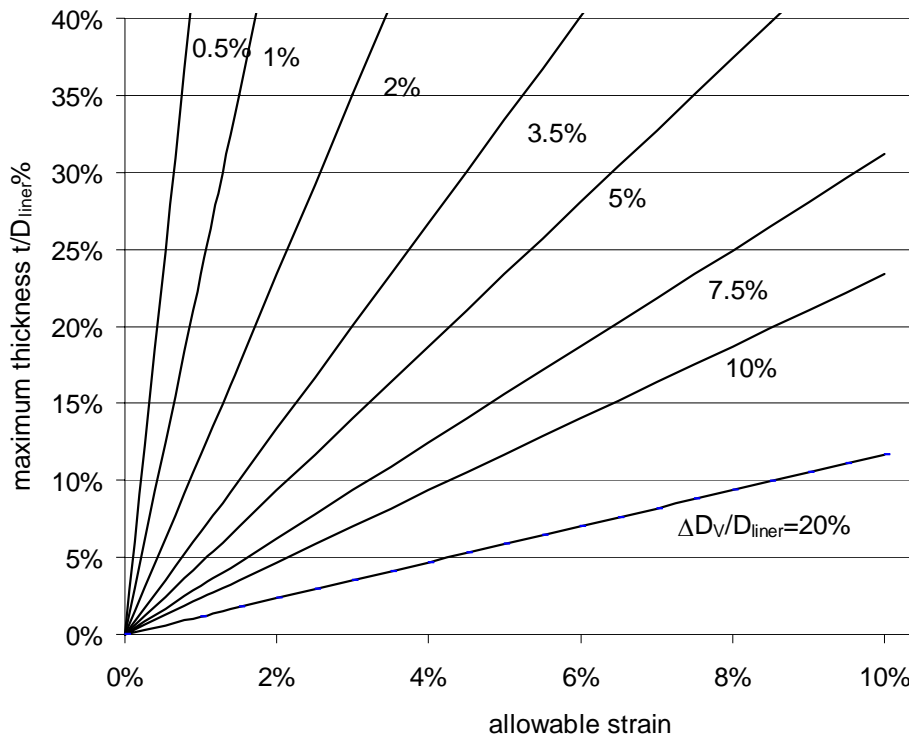


Figure 13. Maximum liner thickness as function of the pipe deformation and allowable strain.

6.3 Reductions in resistance to bending

Law and Moore (2007) examined the local bending that results from contacts between pipe and liner at the crown and invert, Figure 3c, and demonstrated that bending strains in the liner can be effectively calculated using the solution for a ring under parallel plate loading:

$$\varepsilon_{cr} = \varepsilon_{in} = \pm \frac{\Delta D_v c}{2\pi \bar{R}_{liner}^2 \left(\frac{\pi}{8} - \frac{1}{\pi} \right)} = \pm \frac{2.139 \Delta D_v c}{\bar{R}_{liner}^2} \quad [12]$$

where the liner has mid-surface radius of \bar{R}_{liner} , and c is the distance from the mid-surface to the extreme fiber responding in tension. Here, the change in vertical pipe diameter ΔD_v is assumed to take place in some sections of the sewer after the liner is inserted. The value of ΔD_v determined from a CCTV inspection of the deformed pipe prior to lining, Moore (2005), should be used if, at the time of liner construction, there is a possibility of similar amounts of soil deterioration behind segments of unfractured pipe. Figure 13 illustrates how the percent change in vertical diameter and allowable strain for the polymer liner control the maximum thickness of a plain liner where $t=2c$. This bending limit state sets an upper bound to liner thickness, since greater liner thickness increases distance to the extreme fibres.

The nature of liner bending within corroded metal culverts has not yet been studied. New work funded by the combined U.S. DOTs as NCHRP Project 14-19 will involve tests at Queen's University on metal culverts after repair and should establish the nature of live and earth load effects on tight fitting and other liners.

7. EXAMPLE CALCULATIONS FOR FRACTURED RIGID SEWERS

The two sewer examples in Figures 1 and 3 are examined here to show the effect of pipe and soil deterioration on liner design. Table 1 contains the key geometrical and material variables (internal diameter, wall thickness, burial depth, backfill, liner modulus and strain capacity).

Table 2 contains details of:

- (a) deflection estimated from buried flexible pipe theory, Eq. [1] and Figure 5
- (b) change in horizontal pipe diameter observed in the CCTV video
- (c) design modulus obtained from soil type and the database of McGrath et al. (2002)
- (d) equivalent uniform modulus after soil degradation back-calculated using (b) in Eq. [1]
- (e) soil degradation index *SDI* calculated using (a) and (b) in Eq. [3]
- (f) approximate void angle α calculated using (e) in Eq. [5]; lower bound parameters were used for the fine grained soil (ML90), upper bound values for the granular soil (SW95).

These calculations demonstrate the clear difference between the deflections expected if this sewer pipe were to fracture but retain the original soil support conditions, column a, and those observed, column b. The substantial reductions in equivalent soil modulus (*SDI* values of 32% and 9%) correspond to the original soil with voids that contact over angles of 56° and 69° at the springlines. These produce large increases in bending moment that explain the pipe fracture.

Table 3 illustrates how the acceptable liner thicknesses change with sewer damage:

- (g) fluid buckling pressure correction factors $R_f R_\Delta$ for a perfect circular sewer, 1.0
- (h) fluid buckling pressure correction factors $R_f R_\Delta$ for a liner in the damaged sewer Eq. [11]
- (i) minimum liner thickness to resist buckling, for factor of safety of 2, using (g) in Eq. [6]
- (j) minimum liner thickness to resist buckling, for factor of safety of 2, using (h) in Eq. [6]
- (k) the maximum liner thickness to ensure bending strains are within the allowable limits, based on deflection for fractured pipes in intact ground, i.e. using (a) in Eq. [12]
- (l) the maximum liner thickness to ensure bending strains are within the allowable limits, based on the deflection observed using CCTV inspection, i.e. using (b) in Eq. [12].

Table 1. Geometry, burial conditions and proposed liner for the example sewers.

	Sewer Pipe		Backfill Soil			Liner	
	ID mm	thickness mm	depth m	type	unit weight kN/m ³	modulus MPa	max. strain
Canada	305	30	3	ML90	20	1500	1.0%
Germany	800	75	5	SW95	22	1500	1.3%

Table 2. Displacement, modulus and void characteristics calculated for the example sewers.

	% deflection		modulus MPa			erosion void angle (f)
	$\Delta D_H/ID$ flexible (a)	$\Delta D_H/ID$ CCTV (b)	design soil (c)	degraded soil (d)	SDI (e)	
Canada	2.17%	7%	5.2	1.6	32%	56°
Germany	0.95%	11%	22	1.9	9%	69°

Table 3. Example sewer buckling factors and liner thicknesses for the two limit states

	buckling factor $R_q R_A$		minimum t mm		maximum t mm	
	perfect shape (g)	actual (h)	perfect shape (i)	actual (j)	perfect soil (k)	actual (l)
Canada	1	0.68	3.0	3.6	32.3	10.2
Germany	1	0.54	10.0	13.3	255.9	22.1

8. CONCLUSIONS

Typical damage in deteriorated rigid sewers is discussed, including the impact of soil erosion. Finite element calculations explain the rigid pipe fracture process, where increases in bending moment and subsequent fractured pipe deformations increase as erosion voids develop. The effect of invert corrosion in corrugated metal culverts has also been calculated. These show factors of safety against yield in the corroded zone that decrease linearly as thickness decreases. The effect of corrosion on factor of safety against buckling was also reported. Tight fitting liners within fractured rigid sewers have decreased ability to withstand the surrounding water pressure, given the approximately oval shape and the wavy imperfection in the liner as it crosses the fractures at the invert and crown. The tight fitting liner also experiences tensile stress and strain induced by bending at the crown and invert, which limits the maximum liner thickness.

9. REFERENCES

- El Taher, M. and Moore, I.D. (2008). Finite element study of corroded metal culvert stability, TRB Annual Conf., Washington D.C., January 14-17, 32pp (to appear, Transp. Res. Rec.).
- El Sawy, K. and Moore, I.D. (1997). Parametric study for buckling of liners: effect of liner geometry and imperfections. In: Trenchless Pipeline Proj. Pipeline Div., ASCE, 416-423.
- Law, T.C.M. and Moore, I.D. (2007). Numerical modeling of tight fitting flexible liner in damaged sewer under earth loads, *Tunnelling and Underground Space Tech.*, 22, 655–665.
- McGrath, T.J., Moore, I.D., Selig, E.T., Webb, M.C. and Taleb, B. (2002). Recommended Specifications for Large-Span Culverts. NCHRP Report 473, 39pp plus Appendices.
- Moore, I.D. (2005). Buried Infrastructure Repair Using Liners: Construction Techniques, Structural, and Geotechnical Issues”, 11th Int. Symp. on Structural and Geotechnical Eng., Cairo, Egypt, May
- Spasojevic, A.; Mair, R.J., and Gumbel, J.E. (2007) Centrifuge modelling of the effects of soil loading on flexible sewer liners, *Géotechnique*, 57(4), 331-341.
- Tan, Z. and Moore, I.D. (2007) Effect of backfill erosion on moments in buried rigid pipes, Transportation Research Board Annual Conference, Washington D.C. January, 29pp.
- Tan, Z. (2007) Effect of soil voids on sewer repair using liners, MSc Thesis, Department of Civil Engineering, Queen’s University at Kingston, Ontario, Canada.